ON EXPLOSIVE BLAST WAVES AND SNOW: Insights from measurements with time-synchronized air pressure sensors and geophones

Benjamin Meier*[1], Samuel V. Verplanck[2]

[1]*Wyssen Avalanche Control AG, Reichenbach, Switzerland*
[2]*Montana State University (MSU), Norm Asbjornson College of Engineering, Bozeman, Montana, USA*

ABSTRACT: In a project funded by the Transportation Avalanche Research Pool (TARP), we investigated the interaction between explosive blast waves and the snowpack to improve shot placement and charge sizing for avalanche mitigation. We employ high-resolution, time-synchronized measurements of air pressure above the snow surface and near-surface snow motion using geophones embedded in the snow.

Field experiments conducted in January 2026 on the Jungfraufirn, a glacier near the Jungfraujoch, Switzerland (3500 m elevation), provided a flat-field winter test designed to minimize terrain reflections and isolate the interaction between the blast wave and the snowpack. Eight explosive charges were detonated above, on, or beneath the snow surface. Three different types of explosives were tested.

We show that the blast wave propagates at the speed of sound in air and that peak over-snow pressure decays according to a power law. Higher frequency components attenuate more rapidly. The timing of the over-snow pressure signal aligns with the peak snow velocity, indicating that local air–snow coupling dominates over wave propagation within the snowpack.

Geophone measurements reveal that the oscillation frequency of the snow response is similar across all tested charges. In contrast, oscillation magnitude is strongly correlated with the amplitude of the initial shock front.

Although based on one snowpack, these high-resolution, coupled measurements and analysis represent an important step toward a mechanistic understanding of blast wave–snow interactions that can inform future avalanche mitigation strategies.

KEYWORDS: Explosives, Avalanches, Pressure, Shockwave, Experiments, Geophones

1. INTRODUCTION

The project overall aims to better understand how the blast wave of explosions interacts with the snowpack. Although explosives have long been used to intentionally trigger avalanches, the increased development and implementation of Remote Avalanche Control Systems (RACS) have sparked important questions related effective blast radii, optimal charge placement, effect of different explosive types, and effect of different snowpacks. A complete, mechanistic understanding of the interaction between an explosion, snow, and subsequent avalanche release has eluded many researchers although progress has been made Gubler (1976), Johnson (1980), Binger and Miller (2016), Simioni (2017), and Seitz (2021).

In this proceeding, we present our findings using high-fidelity, time-synchronized observations of air pressure and coupled snow velocity at a test site chosen to minimize compounding factors such as reflections off the ground, cliffs, and asymmetry of slopes.

* *Corresponding author address:*
Corresponding author address:
Benjamin Meier, Wyssen Avalanche Control AG
3713 Reichenbach, Switzerland;
tel: +41 33 676 76 64;
email: beni@wyssen.com

2. METHODS

The tests were performed on a single test day, 13th January 2026 on a large flat area of the Jungfraufirn, a glacier near the Jungfraujoch, Switzerland (Figure 1). The test site is at 3500m (11500ft) elevation, the atmospheric pressure was at 669.4hPa.

2.1. Snow conditions

The top 155 cm of snow was observed according to Fierz et al. (2009). The profile ranged in density from 220 to 470 kg m^{-3} with a mean of 340 kg m^{-3}. The top 32 cm were identified as decomposing and fragmented particles (4F to 1F+), followed by a 17 cm rounded grain layer (1F+) on top of a 2 cm melt-freeze crust (K). Directly below the crust was a notable 18 cm layer of facets (4F). Below this faceted layer was a mixture of faceted crystals, melt forms, and rounded grains that ranged in hand hardness from 1F+ to K. Below the observed snow profile is firn (roughly 50 m) and glacial ice (roughly 200m) based on personal communication with a Jungfraujoch employee. The detailed pit profile can be found on snowpilot.org (Pit ID 78994).

https://doi.org/10.15788/1790098476

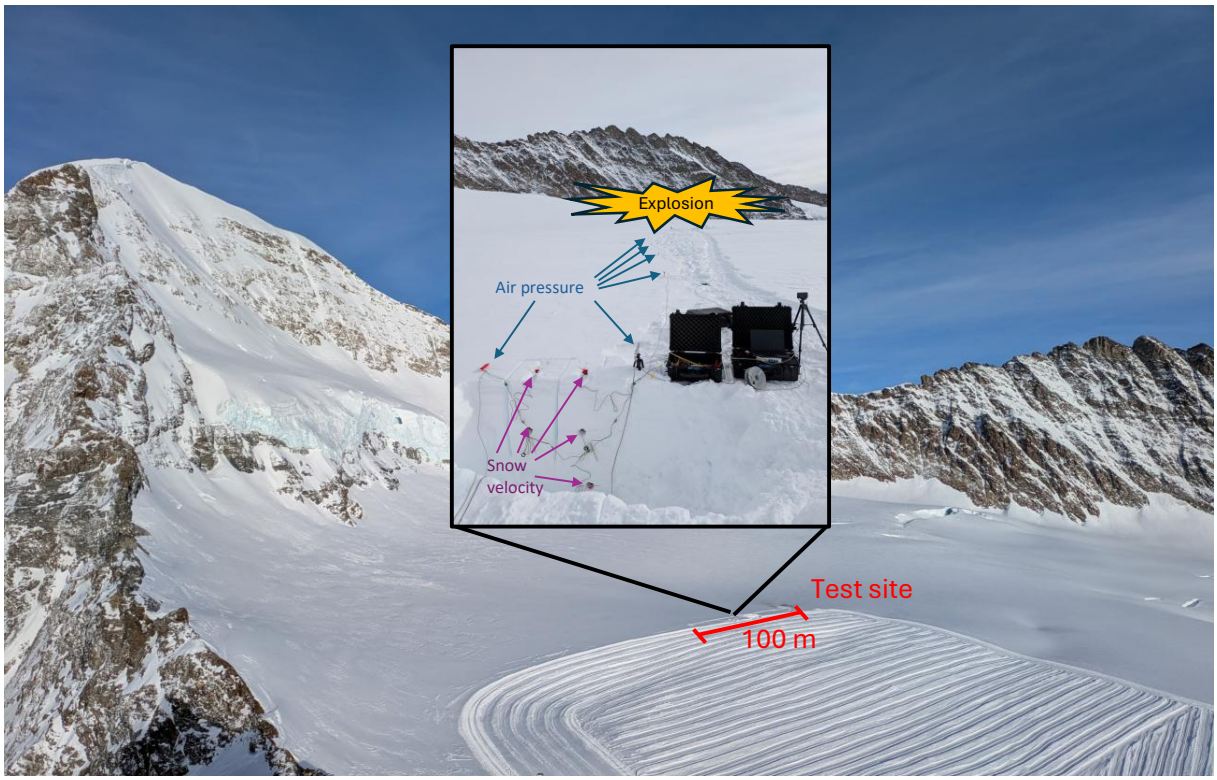


Figure 1: Experiments took place on a flat area of the Jungfraufirn glacier. This location minimized interactions with surround terrain to isolate the interaction between a blast wave and snow.

Table 1: Properties of explosives used in this experiment Tovex Société Suisse des Explosifs SA (2020b), Wyssen Wyssen Avalanche Control AG (2026), and Plastex Société Suisse des Explosifs SA (2020a) as well as Pentolite Dyno Nobel Inc. (2026) and Comp-B J. Köhler (2008). Velocity of detonation (VoD), heat of detonation (HoD), and gas volume are shown.

Product	VoD (m/s)	HoD (kJ/kg)	Gas Volume (L/kg)
Tovex AV	4500	3500	950
Wyssen 2K	4300	4000	920
Plastex	7500	5400	860
Pentolite	7300	5200	750
Comp-B	8000	5300	890

2.2. *Explosives*

Three different explosives were tested. Two of them are commonly used in avalanche control: Wyssen 2K and Tovex AV. The third explosive, Plastex, is not typically used for avalanche control, but has similar properties as the military explosives (Comp-B and Pentolite) sometimes used for avalanche control in the US (Table 1).

The charge sizes were selected such that they represent charges one would typically find in avalanche blasting. The full sized Wyssen 2K, Tovex 5kg and Plastex 5kg charges represent typical explosives used in Wyssen Remote Avalanche Control Systems (RACS). The Plastex 1kg charges are intended to represent the 2lb pentolite-sticks (two-pounder) often used as hand charges by ski-patrollers in the US.

2.3. *Charge placement*

The charges were deliberately placed in different locations relative to the snow surface. The default setup was on a bamboo-stick, detonating about 1.8 m above the snow. Some charges were laid on the snow surface, which could happen in a typical hand-charge scenario. Other charges were buried in the snow at a depth of 50 cm. This represents a charge thrown in the snow from a helicopter or potentially a hand charge that sinks into a deep fresh snowpack. The legend in Figure 3 details each test.

2.4. *Sensors*

Air pressure was measured using purpose-built pressure sensors, sampling at 23437.5Hz with a resolution of 24-bit. The sensors were placed at 16.5m, 20m and then every 5m up to 100m horizontal distance from the detonation (i.e. ground

zero).

Vertical motion of the snow was observed with an array of geophones recording at the same sampling frequency and resolution. The geophones were placed in three snow pits at 16.5m, 50m and 100m. Five geophones were placed in each snowpit. Three of them were installed at depths of 3.5cm (barely covered), 50cm and 100cm. Two additional geophones were placed at 3.5cm and 50cm but in a patch of snow that was cut free on all four sides to create an ”isolated” column of snow similar to a Compression Test Jamieson and Johnston (1996).

All sensors were connected to a central controller with a CAN-Bus. Prior to each detonation a synchronization message synchronized all the sensors to a timing-accuracy of one sample or better ($\Delta t \leq 42\mu$s). After each detonation, the recording was then stopped and the data downloaded to the controller and subsequently to the connected laptop.

The pressure readings were calibrated to match the measurements from a reference setup with Kistler sensors (Model 6233A0025) placed at 16.5 m, 50 m, and 100 m.

3. RESULTS

3.1. Raw observational data

Observed air pressure from the blasts showed a steep shock front leading to a peak overpressure followed by a decay to lower magnitude negative pressure and return to ambient (Figure 2). The curves decay in amplitude as distance increased from ground zero. These air pressure observations are coupled with geophone-based observations of velocity at the surface, 50 cm deep, and 100 cm deep. The snow motion events align in time with the arrival of the shock front. The geophones closest to the detonations at 16.5 m exceeded their range of measurement ($\pm$ 86.96 mm/s) in most recordings, the sensors at 50m in some and the sensors at 100 m for none of the detonations.

3.2. Wave speed in air

All tests indicated that the peak overpressure from the blast wave traveled at the effectively constant speed of 323.0 $\pm$ 1.4 m/s which is similar to the speed of sound in air, a_x 326 m/s ($a_x = \sqrt{\gamma RT/M}$, γ = 1.4, R = 8.314 J/mol/K, T = 264.5 K, and M = 0.029 kg/mol).

Kinney (1985) suggests that the speed of the shock front from detonations in air, while starting with a speed substantially above the speed of sound, asymptotically approach the speed of sound according to

$$t_a = \frac{1}{a_x} \int_{r_c}^{r} \left[\frac{1}{1 + \frac{6p^0}{7P_a}} \right]^{1/2} dr \qquad (1)$$

where t_a is the arrival time, a_x is the speed of sound in undisturbed air, p^0 is the peak overpressure, P_a is the atmospheric pressure, r is the radial distance from the explosion, and r_c is the charge radius. Using analytic formulations of peak overpressure for 0.1 kg, 1 kg, and 5 kg of TNT Kinney (1985), Figure 3 shows a speed faster than the speed of sound only for the first few meters then the speed approaches the linear regime which agrees well with our data.

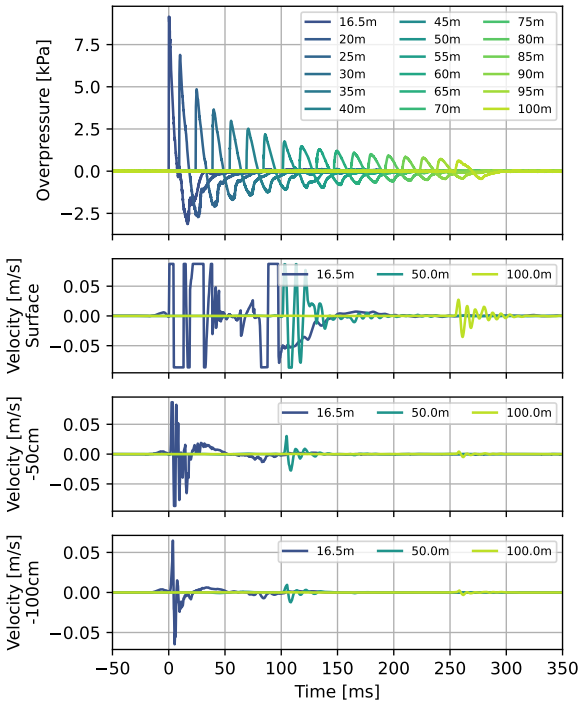


Figure 2: Raw air pressure recordings for ”Tovex 5kg above snow” and the corresponding velocity measurements at three different sensor depths. All the recordings are synchronized and aligned such that the first pressure-sensor at 16.5m has the peak at $t = 0$. Positive velocity is downward, i.e. into the snowpack.

3.3. Peak overpressure decay

As air pressure from the explosions were measured at different distances, we have 18 of peak-overpressure readings for each explosion less any sensor malfunctions. The values span across a

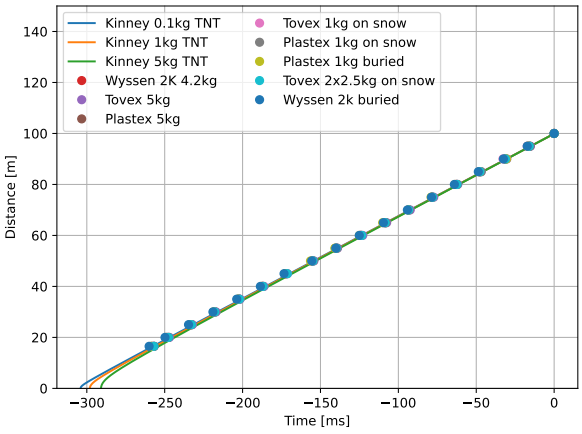


Figure 3: Theoretical arrival times according to Kinney (1985) and recorded arrival times of peak overpressure at each location for each test. Data are aligned at the farthest point from ground zero (100m) to show subtle differences closer to the origin.

large dynamic range, 25Pa to 12.5kPa, and are therefore plotted on a logarithmic axis (Figure 4). The power-law $p^0 = A\,r^b$, where r is the radial distance from ground zero, and A and b are fit parameters, was fitted to the peak overpressure data; the fit parameters shown in Table 2.

The power laws were subsequently used to estimate the distance where the peak pressure is 1kPa, a threshold commonly used in this type of work.

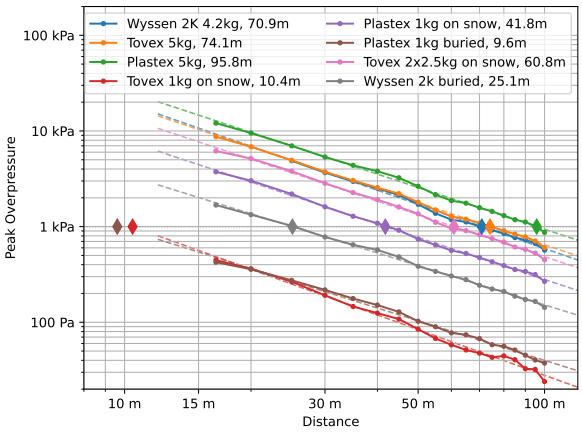


Figure 4: Peak overpressure for each experiment at each sensor location. The dashed lines represent the power laws. The diamond markers indicate the distance where the power-law crosses the 1kPa threshold, that distance is also indicated in the legend.

While the charge size and charge type were shown to have negligible influence on the speed of the wave, the explosive type, size, and placement show influence on peak overpressure with airblasts having the highest amplitudes. Despite the differences in amplitudes, the peak overpressure values decay at a similar rate. This is consistent with the findings of Gubler (1976) and Seitz (2021).

When comparing different explosive charges Kinney (1985) suggests that we should look at the total energy of an explosive charge. The total energy (usually expressed in kg TNT) let's us predict the characteristics of the blast wave (e.g. peak overpressure) at any distance.

The scaling law (Hopkinson (1915) and Cranz (1926)) states that the effect of all explosives is the same when the distances are scaled according to $z = r/\sqrt[3]{W_{\text{TNT}}}$, where r is the actual distance, z the scaled distance and W_{TNT} the yielded energy expressed in kg of TNT.

As we do not know the energy density of some of the explosives and further do not know the effect the charge placement (e.g. buried charge) has on the effective energy yield, we cannot use this to predict the blast wave parameters in our case.

But by using the scaling law in reverse we can estimate the perceived yield for the used charges with our particular placements. The observed overpressure of the "Tovex 5kg above snow" charge aligned well with the predicted values for 5kg TNT at the scaled distances. But for the smaller charges or more disadvantageous placements the data is better aligned with a power law. By applying the reverse scaling law such that the data aligned with the power law, we can estimate the perceived yields (Table 3).

A buried charge has a less widespread effect than the same charge positioned at the snow surface (see values for Plastex 1kg). Similarly the effect of 5kg of Tovex positioned 1.8 m above the snow surface has a more widespread effect than the same amount of Tovex (2x2.5kg) on snow.

Using the obtained 1kPa radii (Figure 4) we can estimate the effect of charge placement as follows. The Tovex 1kg on snow charge has a comparatively small yield, probably caused by the charge not fully detonating as it was built using 5 sticks of 200g each. We excluded these values for this analysis:

- On snow (Tovex 2x2.5kg on snow) has a relative effective radius (compared to Tovex 5kg) of 82.1%
- On snow (Plastex 1kg on snow) has a relative effective radius (compared to Plastex 5kg,

Table 2: Power-law fits $p^0 = A\,r^b$ per experiment. δ_n is the 1σ standard error of the slope b and N is the number of air pressure observations used in the fit.

Charge	Placement	b	δ_n	A	R^2	N
Wyssen 2K 4.2kg	above snow	-1.528	0.026	671.9	0.996	16
Tovex 5kg	above snow	-1.464	0.016	546.4	0.998	18
Plastex 5kg	above snow	-1.448	0.018	739.1	0.998	18
Tovex 1kg	on snow	-1.584	0.033	41.2	0.993	18
Plastex 1kg	on snow	-1.458	0.014	230.4	0.999	18
Plastex 1kg	buried	-1.374	0.023	22.4	0.996	18
Tovex 2x2.5kg	on snow	-1.457	0.017	398.2	0.998	18
Wyssen 2k	buried	-1.363	0.015	80.8	0.998	18

Table 3: Perceived yield, W_{TNT}, for each experiment obtained by fitting the values to a power law. For the Tovex 5kg charge the yield was assumed to be 5kg as a reference.

Experiment	W_{TNT}
Tovex 1kg on snow	0.009
Plastex 1kg buried	0.015
Wyssen 2k buried	0.225
Plastex 1kg on snow	0.897
Tovex 2x2.5kg on snow	2.758
Wyssen 2K 4.2kg	4.493
Tovex 5kg	5.000
Plastex 5kg	10.565

scaled by $\sqrt[3]{\frac{W_1}{W_2}} = \sqrt[3]{\frac{1}{5}} = 0.585$ because we are comparing charges of unequal sizes) of 74.6%

- Buried (Wyssen 2K buried) has a relative effective radius (compared to Wyssen 2K 4.2kg) of 35.4%
- Buried (Plastex 1kg buried) has a relative effective radius (compared to Plastex 5kg, scaled by $\sqrt[3]{\frac{1}{5}} = 0.585$) of 17.2%

The Plastex charge, when detonated in air, gains energy from burning its excess fuel with oxygen from the atmosphere. This process is minimal when the charge is detonated in snow. For that reason, placing Plastex inside the snowpack is additionally disadvantageous.

When we assume for a charge placed on snow that half of the energy dissipates completely in the snow, the scaling law gives us a relative effective radius of ($z_2 = z_1 \sqrt[3]{0.5}$) 79%, which is consistent with the ratios from our experiments.

For the scaling law to give a relative radius of 35.4% one needs to assume that 95% of the energy is dissipated in snow ($\sqrt[3]{0.05} \approx 36.80.\%$).

3.4. *Frequency content of air pressure observations*

In the previous section we only looked at the peak overpressure, but when we look at the whole time series of overpressure, we can see that the signal with its sudden and sharp increase in pressure must contain many different frequencies. Looking at the same signal at a more distant sensor, the steepness of the shock front has reduced as well as the peak overpressure (Figure 2).

By taking the Fourier transform of the air pressure measurements, we ascertained the relative amplitude of the frequency content of the blast wave at different locations (Figure 5). The relative amplitudes of frequencies tended to decrease as distance from ground zero increased. Furthermore, there is a larger relative decay in the higher frequency components in this range than the lower frequency components. This observed attenuation is in the order of 20-30dB in 100m (1kHz) and thereby substantially larger than atmospheric attenuation which is in the order of 0.5dB/100m, Bass et al. (1995). This increased attenuation is likely a direct result of the blast wave-snow interaction.

3.5. *Correlation of overpressure and velocity*

The blast wave passing over a geophone location coincides with largest magnitude of vertical velocity (Figure 2). This is further illustrated by plotting peak downward velocity (positive) against peak overpressure recorded by the overlying air pressure sensor (Figure 6). If the dynamic range of the geophone was exceeded, then that data was neglected from this analysis.

The power laws ($v_{peak} = A_{vel}(p^0)^{b_{vel}}$) obtained from the observed relationship peak velocity and

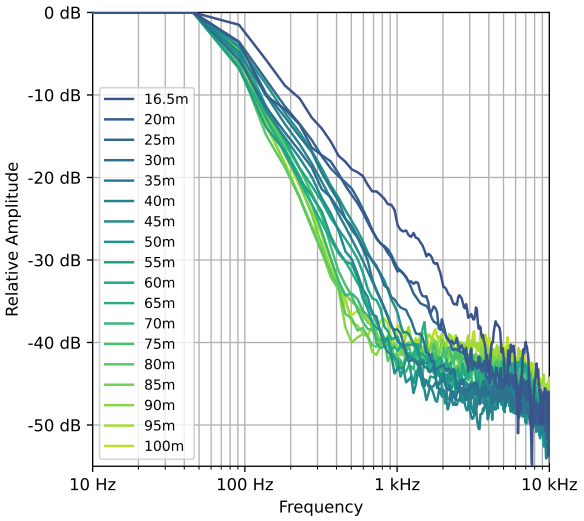


Figure 5: Frequency content of the air pressure observations from the Tovex 5kg blast above snow. The magnitudes are normalized by aligning the maximum with 0dB.

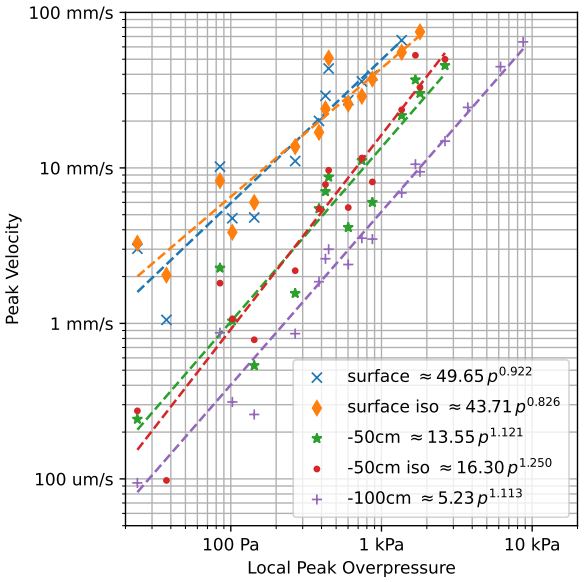


Figure 6: Recorded peak velocity, v_{peak} plotted against the peak overpressure, p^0, measured at the respective distance. The plotted lines are fitted to power laws.

peak overpressure values (Figure 6) have a mean exponent of $b_{vel} = 1.05 \pm 0.15$. This seems plausible as we can expect linear behavior at the observed amplitudes and Gubler (1976) and others linked peak overpressure with velocity.

From the gain coefficient, A_{vel}, of the power-law gives us an order of magnitude on the attenuation with snow depth. The velocity amplitude was observed to be reduced by a factor of ≈ 3.23 per 50cm which equates to $ln(3.23^2) = 2.35$Np/m (Neper per meter). While this nicely calculates to a factor of 1/10th $(1/3.23^2)$ per m, it is probably coincidental and only valid for our particular analysis with our particular snowpack.

The same analysis was done for impulse for the positive portion of the overpressure curve. For impulse the correlation was similar but with a larger standard deviation of the values against the power-law. As duration gets larger with increasing distance the correlation there was very small. We therefore concentrated on the peak overpressure vs. peak velocity relationship.

A low magnitude geophone signal preceding the arrival of the blast wave (non-zero velocity in Figure 2 where $t < 0$) can occasionally be detected. This is consistent with Gubler (1976) and Simioni (2017), who also measured the seismic wave arriving before the larger amplitude wave that is induced locally.

3.6. *Similarities in velocity readings for all detonations*

Interestingly, while the amplitude of the velocity curves correlates with the overpressure amplitude, when normalized by velocity amplitude, the velocity signals look very similar. For example, looking at the velocity readings from the geophone 50 m from ground zero and 50 cm into the snow (Figure 7) we see the same characteristic oscillation for each of the detonated charges. For example, the positive phase portion of the overpressure for the "Tovex 5kg" and "Tovex 1kg" are notably different, the amplitude-normalized shape of the velocity waveform is quite similar (Figure 7). This is a strong indication that the oscillation is characteristic for the snowpack while the amplitude is driven by the amplitude of the overpressure.

3.7. *Transfer function modeling*

As we have time-synchronized measurements of overpressure in air and velocity in snow, we are in a unique position to develop a transfer function.

Using the Laplace transform $\mathcal{L}\{\cdot\}$, with pressure $P(s) = \mathcal{L}\{p(t)\}$ and velocity $V(s) = \mathcal{L}\{v(t)\}$, the transfer function is defined as:

$$H(s) = \frac{V(s)}{P(s)} = e^{-s\tau} \sum_{i=1}^{3} \frac{K_i s}{s^2 + 2\zeta_i \omega_i s + \omega_i^2} \quad (2)$$

Using only one lag parameter $\tau = 0.65$ms plus 3 poles, each characterized by their undamped natural frequency ω_i, the damping ratio ζ_i and the gain K_i, we were able to model the observed behavior quite well. This was done using all the data

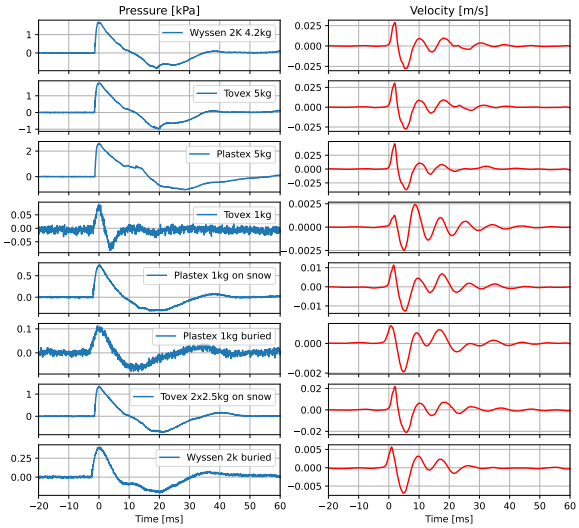


Figure 7: Pressure recording and the corresponding stress-wave (50cm depth) recording at 50m for each detonation. The waveform of the stress-wave looks fairly similar for each detonation while the pressure wave has significant variance in the duration of the positive phase.

in Figure 7 (pressure and velocity at 50m), to fit the transfer functions parameters to the values shown in Table 4.

Table 4: Parameters for the transfer function equation (2) found by fitting the model to the data. The natural frequencies $f_{0,i}$ are defined as $f_{0,i} = \frac{\omega_i}{2\pi}$.

Mode	K_i	$f_{0,i}$	ζ_i
1	5.581	121.6	0.1179
2	-5.398	326.2	0.1201
3	-0.389	42.0	0.1873

The continuous-time transfer function was discretized using the bilinear (Tustin) transform, yielding a discrete-time representation in the (z)-domain. The resulting model was then used to simulate the snow's response in the time domain to arbitrary pressure signals. Figure 9 shows good agreement of the model output with the recorded velocity when the entire measured overpressure wave is input.

That we can fit a linear transfer function between pressure and velocity data agrees with the earlier finding of the linear relationship between overpressure amplitude and velocity amplitude (Figure 6).

The prominent peak in the transfer functions bode-plot (Figure 8) is in good agreement with the observation, that the velocity waveform is mostly invariant to the waveform of the pressure wave (Figure 7).

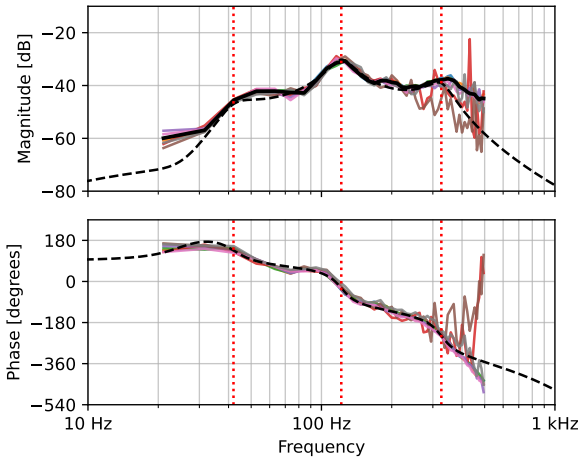


Figure 8: Obtained transfer function $H(s)$ (dashed black line) in a bode-plot. The numerical estimation of the transfer function per blast was averaged into one transfer function (solid black line). Then the three poles (shown as red dotted lines) were searched such that the model fits the averaged transfer function. The colored lines are the magnitude and phase of the geophone recordings.

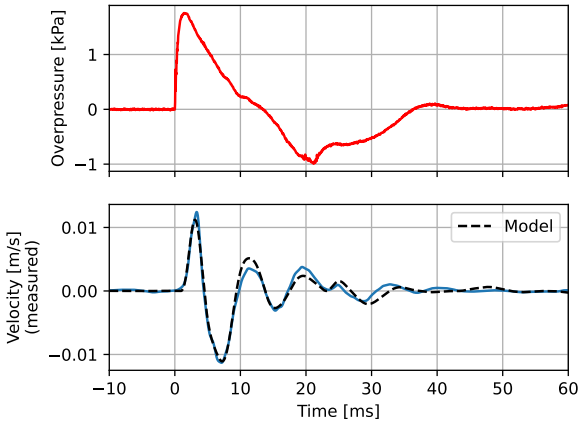


Figure 9: Transfer function response (model) has good agreement with snow velocity observations (50m, 50cm depth) when the entire overpressure waveform at 50m (red line) is the input.

Our model allows us to calculate the theoretical response of the snowpack at this particular location to an artificial pressure signal. We can use it to estimate what velocity would be expected if only part of the pressure wave arrived at the snow and thereby find out which part of the wave causes most of the movement of snow.

To estimate how much of the effect comes from the first steep pressure increase we held the pressure signal for the model input at $t = 1.5$ms, the result is shown in Figure 10. The modeled velocity generally agrees with observed, but with some error particularly apparent in the negative regions.

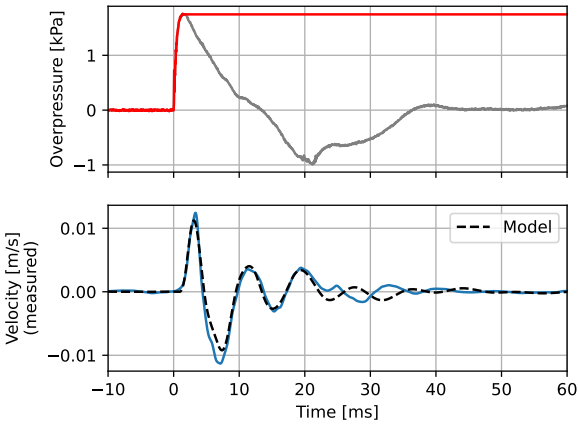


Figure 10: Modeled velocity from a pressure wave (red line) that has the first increase of the original pressure measurement (gray), then keeps at the peak pressure.

If we feed the whole positive overpressure phase into the model (Figure 11) by holding the signal after $t = 12.5$ms we see that the largest part of the positive overpressure phase has only very limited effect on the velocity in snow.

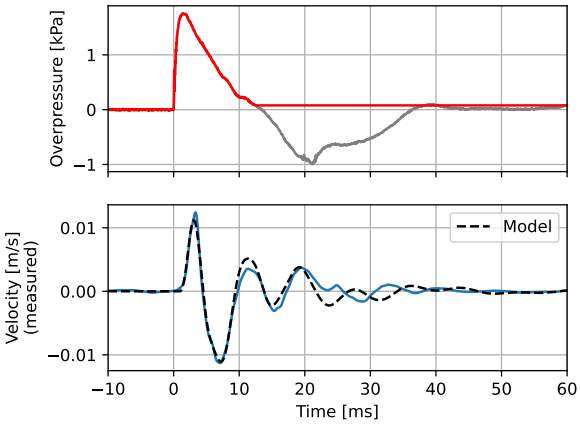


Figure 11: The calculated velocity (denoted as model) from a theoretical pressure wave that remains near zero after the positive overpressure phase.

4. DISCUSSION

4.1. *Relevance for avalanche mitigation*

Across all the explosive configurations tested, peak overpressure on the snow surface directly above the geophones showed a strong correlation with peak snow velocity indicating that the blast wave through air causes more widespread disturbance in snow rather than a seismic wave transmitting through the snow. This provides further confirmation that for a given charge size, air blasts have the widest area of effect, followed by surface blasts, followed by subsurface.

When comparing the velocity readings for the different test configurations, we observed very similar profiles of snow motion but with different amplitudes. This indicates that the given snowpack had a characteristic response to loading from the shock front, independent of the type of explosive that caused that shock front.

4.2. *Limitations and future work*

These experiments were performed on a single test day in one location. It therefore does not allow us to differentiate between snow conditions. More observations are recommended in different snow conditions to further illuminate the interaction between blast waves and snow. For example, an interesting analysis would be to link transfer function parameters, namely natural frequency, with snowpack properties across a range of snowpacks.

The tests were conducted in a flat snow field with minimal terrain interactions. This was intentional to isolate the snow-blast wave interaction. Avalanches occur on slopes and in seasonal snowpacks that are on the order of meters deep, rather than hundreds of meters. Interactions between the blast wave, snow, and surrounding terrain are all critical for a wholistic understanding of avalanche release from explosions.

The power laws ascertained for peak overpressure decay are not without limitations. Peak overpressure was defined as the maximum pressure value during the recording, which may not directly coincide with the first peak, particularly for pressure readings that were lower in magnitude with a smaller gap between signal and noise. Furthermore, observations were made from 16.5 m to 100 m. These power laws are not expected to be accurate in closer and farther distances than those tested.

The transfer function used in this analysis was only defined using geophones 50 cm depth at 50 m distance from ground zero and the air pressure readings at 50 m. The transfer function is expected to vary at other distances, depths, and snowpacks.

The geophone analysis thus far has been limited to velocity. Snow failure criteria are often tied to stress and strain rate Schöttner et al. (2026). For further analysis, we recommend ascertaining strain and strain rates using the coupled geophone observations and stresses by applying appropriate constitutive relationships. Furthermore, only

vertical motion was captured, future studies could capture radial motion to acquire 2D motion.

5. CONCLUSIONS

In this study we observed time-synchronized air pressure and snow velocity from different explosives that were detonated above, on, and within the snow. The study took place on a flat part of the Jungfraufirn glacier far enough away from surrounding terrain features that would cause a significant reflection with the intent to isolate the blast wave-snow interaction.

- The blast waves for all experimental configurations propagated at the speed of sound in air which agrees with theoretical predictions.
- The peak overpressure decay is well represented by a power law. Although the amplitudes vary with the different explosive configurations, the rate of decay is similar across all test configurations.
- Higher frequency components of the air pressure readings decayed with distance from ground zero.
- Peak snow velocity aligned with peak overpressure, indicating that snow motion was primarily driven by the over snow air pressure rather than seismic wave transmission through the snow from ground zero.
- Magnitude of peak snow velocity and peak overpressure showed a strong positive correlation, whereas normalized velocity waveforms showed similarity in shape across all test configurations. In addition, the correlation with impulse was less consistent and the velocity waveform is well-represented by the initial overpressure loading according to transfer function modeling. Therefore, we conclude the amplitude of the peak overpressure is the primary driving factor for snow's response to the explosive configurations tested.

ACKNOWLEDGEMENTS

Thanks to Andreas Egger, Jamie Yount and the people of Jungfraubahnen as well as TARP to support the experiments.

REFERENCES

Bass, H. E., Sutherland, L. C., Zuckerwar, A. J., Blackstock, D. T., and Hester, D. M. (1995). Atmospheric absorption of sound: Further developments. In: The Journal of the Acoustical Society of America 97.1, pp. 680–683. ISSN: 0001-4966. https://doi.org/10.1121/1.412989. eprint: https://pubs.aip.org/asa/jasa/article-pdf/97/1/680/9433455/680_1_online.pdf.

Binger, J. B. and Miller, D. A. (2016). Soft and Hard Slab Snow Dynamic Response to Explosives Used in Avalanche Hazard Mitigation. In: Journal of Cold Regions Engineering 30.2, p. 04015003. ISSN: 0887-381X, 1943-5495. https://doi.org/10.1061/(ASCE)CR.1943-5495.0000096.

Cranz, C. (1926). Lehrbuch der Ballistik. Springer-Verlag, Berlin.

Dyno Nobel Inc. (2026). TROJAN GEOPRIME dBX High Performance Pentolite – Technical Data Sheet. Product data sheet.

Fierz, C., Armstrong, R., Durand, Y., Etchevers, P., Greene, E., McClung, D., Nishimura, K., Satyawali, P., and Sokratov, S. (2009). The International Classification for Seasonal Snow on the Ground. In: UNESCO, IHP–VII, Technical Documents in Hydrology, No 83; IACS contribution No 1, p. 80. ISSN: 00201383.

Gubler, H. (1976). Künstliche Auslösung von Lawinen durch Sprengungen. In: Mitteilungen des Eidgenössischen Institutes für Schnee- und Lawinenforschung.

Hopkinson, B. (1915). Experiments on the Design of Bombs. In: British Ordnance Board Minutes 13565.

J. Köhler R. Meyer, A. H. (2008). Explosivstoffe. Wiley-VCH, Inc.

Jamieson, B. and Johnston, C. (1996). "The Compression Test for Snow Stability". In: International Snow Science Workshop. Banff, Alberta, Canada, pp. 118–125.

Johnson, J. B. (1980). A Model For Snow-Slab Failure Under Conditions Of Dynamic Loading. In: Journal of Glaciology 26.94, pp. 245–254. ISSN: 0022-1430. https://doi.org/10.3189/s0022143000010789.

Kinney, G. (1985). Explosive Shocks in Air. Springer Science+Business Media, LLC. ISBN: 978-3-642-86684-5.

Schöttner, J., Piecuch, M., Rosendahl, P. L., Walet, M., Adam, V., Weißgraeber, P., Schweizer, J., and Van Herwijnen, A. (2026). Testing the Strength of Buried Surface Hoar Weak Layers Under Combined Compression and Shear Loading. In: Geophysical Research Letters 53.7, e2025GL120870. ISSN: 0094-8276, 1944-8007. https://doi.org/10.1029/2025GL120870.

Seitz, B. (2021). "Measuring Explosive Airblast of Remote Avalanche Control Systems". MA thesis. Bozeman, MT: Montana State University.

Simioni, S. (2017). "The Effects of Explosions on Snow". PhD thesis. ETH Zurich.

Société Suisse des Explosifs SA (2020a). PLASTEX – Auflegersprengstoff: Technisches Datenblatt. Product data sheet. Brig, Switzerland.

Société Suisse des Explosifs SA (2020b). TOVEX Avalanche – Lawinensprengstoff: Technisches Datenblatt. Product data sheet. Brig, Switzerland.

Wyssen Avalanche Control AG (2026). Wyssen 2K® Ladung – Produktdatenblatt. Product data sheet. Reichenbach i.K., Switzerland.